Analysis and Empirical Validation of Visible Light Path Loss Model for Vehicular Sensing and Communication

Hisham Abuella*, Md Zobaer Islam*, Russ Messenger*, John O'Hara*, and Sabit Ekin†
*School of Electrical and Computer Engineering, Oklahoma State University, Stillwater, OK, USA
†Department of Engineering Technology and Industrial Distribution, Texas A&M University, College Station, Texas, USA
Email: {hisham.abuella, zobaer.islam, russ.messenger, oharaj}@okstate.edu, sabit.ekin@tamu.edu.

***Abstract*—Advancements in lighting systems and photodetectors provide opportunities to develop viable alternatives to conventional communication and sensing technologies, especially in the vehicular industry. Most of the studies that propose visible light in communication or sensing adopt the Lambertian propagation (path loss) model. This model requires knowledge and utilization of multiple parameters to calculate the path loss such as photodetector area, incidence angle, and distance between transmitter and receiver. In this study, a simplified path loss model that is mathematically more tractable is proposed for vehicular sensing and communication systems that use visible light technology. Field measurement campaigns are conducted to validate the performance and limits of the developed path loss model. The proposed model is used to fit the data collected at different ranges of incident angles and distances. Further, this model can be used for designing visible light-based communication and sensing systems to minimize the complexity of the Lambertian path loss model, particularly for cases where the incident angle between transmitter and receiver is relatively small.**

***Index Terms*—Visible Light Communication (VLC), Visible Light Sensing (VLS), Vehicle-to-Vehicle Communication (V2V), Channel Modeling, Path Loss, Vehicular Technology, Lambertian Path Loss Model.**

I. Introduction

Wireless communication and sensing systems have experienced many advancements, from the discovery of electromagnetic (EM) waves, to wireless telegraphs and radios, to modern smartphones, connected vehicles and Internet of Things (IoT) devices. All of these new technologies need wireless communication to adapt to the demand for higher bandwidth and to the inflation of data consumption. New technologies increasingly adopt wireless communications with ever higher bandwidth and data consumption to accomplish their purpose. In some systems, like in the vehicular industry, utilizing the radio frequency (RF) technology can be inefficient due to interference, spectrum scarcity, health concerns and power limitations [1], [2]. In recent years, the interest for use of visible light systems to enable wireless connectivity in vehicle-to-vehicle (V2V) and vehicle-to-infrastructure (V2I) links has increased. It is also called as vehicle-to-everything (V2X) communication. This increasing interest is due to the advancements in light-emitting diode (LED) and photodetector (PD) technologies. Moreover, these systems are less costly, highly efficient and can support high data rates. One important requirement for visible light communication is to avoid human perception of flickering at the light source, an easily achievable task by employing intensity modulation faster than 200 Hz [3].

This material is based upon work supported in part by the U.S. Department of Energy, Office of Science, Office of Advanced Scientific Computing Research under Award Number DE-SC0023957. This work was supported in part by the U.S. National Science Foundation under Grants 2323300 and 2323301.

There are multiple studies discussing different implementations of visible light communication (VLC) in V2X applications. Lui *et al.* introduced the idea of enabling Vehicular VLC (V2LC) systems and studied the effect of multiple vehicles and the visible light noise and interference [4]. They considered the reliability and latency requirements to examine the V2LC performance. Multiple studies have demonstrated the VLC systems for outdoor vehicular scenarios. Cailean *et al.* presented a short distance prototype to transmit data using Miller and Manchester coding [5]. Lourenco *et al.* discussed the challenges that outdoor VLC systems face and implemented a prototype that can achieve low data rates in presence of high optical noise levels [6].

In most of the previously mentioned studies, understating the path loss model and estimating the received light power in different positions (different distances) are critical in estimating the theoretical performance limits of VLC systems. Few researchers have studied and analyzed the visible light channel and its path loss model behavior in real world scenarios, which are important and critical parameters to be considered. The Lambertian propagation (path loss) model was adopted by most of the VLC and VLS (visible light sensing) studies [1], [2], [7], [8]. This propagation model works well in indoor scenarios. However, the same model may not work well for visible light communication and sensing in V2X applications.

As a potential solution, some studies introduced empirical path loss models for the outdoor vehicular VLC systems. Cui *et al.* studied an outdoor VLC link using LED traffic lights where the link path loss model is analyzed both theoretically and experimentally [9]. Viriyasitavat *et al.* derived a realistic path loss model for VLC systems using off-the-shelf scooter taillights. The proposed model accurately estimated the received power from the taillight up to 10 meters [10].

979-8-3503-7099-7/24/$31.00 ©2024 IEEE

Turan *et al.* did a frequency domain channel sounding and characterization for a vehicular VLC in different scenarios [11]. A comparison between radio frequency and visible light propagation channels for vehicular communication was presented by Cheng *et al.* in [12]. Recently, there is a shift in the studies to simplify the visible light path loss model for outdoor vehicular scenarios and to verify these models using simulations in ray tracing software, as done in [13]. Moreover, Elamassie *et al.* developed a path loss model for V2V links as a function of distance under different weather conditions and confirmed their models using ray tracing software [14]. In addition to ray tracing tools, Eso *et al.* performed an experimental investigation on the effects of fog on optical camera based VLC. Memedi *et al.* investigated the impact of vehicle type and headlight characteristics on the VLC performance [15]. However, in the aforementioned studies, the proposed models are experimentally tested with only a limited number of static points (2D or 3D) between the receiver and the transmitter.

In this study, a simplified visible light path loss model is proposed, analyzed and empirically validated for outdoor V2I communication and sensing applications. To verify the proposed model, data are collected from field measurements using off-the-shelf LED lights and a PD using a new dynamic channel modeling approach. This model can be used by different studies to decrease the analysis complexity (i.e., increase mathematical tractability), where the Lambertian propagation model would be assumed and the incident angle is small enough. Moreover, the limits of the developed path loss model are provided.

In summary, the main contributions of this study are as follows:

- Proposing and analyzing a mathematically more tractable and simplified visible light path loss model.
- Verifying the proposed path loss model by field measurements using a dynamic channel modeling approach.
- Discussing the limits of the proposed path loss model and dynamic channel modeling approach.

As per our knowledge, this is the first work to provide and verify a simplified visible light path loss model for V2X applications that takes the motion of the vehicle (dynamic channel modeling) into account.

The rest of the manuscript is organized as follows. In Section II, the system model and the experimental setting are provided. In Section III, the developed path loss model and its mathematical proof are given. In Section IV, the comparison and the field measurements are presented. Finally, the conclusions are discussed in Section V.

II. System Model and Experimental Setting

The system model under consideration is shown in the Fig. 1, where θ and w are the incidence angle and the lateral distance between the vehicle and the photodetector (PD), respectively. R and D are the varying longitudinal distance and the actual distance between the vehicle and the PD, respectively. For simplicity, longitudinal distance (R) is referred to as range and actual distance between the vehicle and the PD (D) is referred to as distance between the PD and vehicle for the rest of the paper.

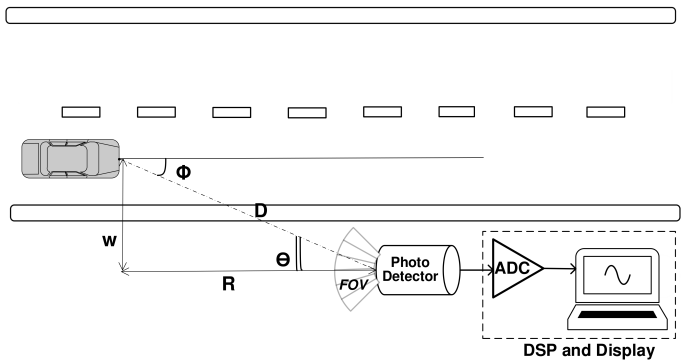

Fig. 1. The system model that is used in the study.

Fig. 2. The experimental setting used for collecting data.

The actual experimental setting used to collect the data is presented in Fig. 2. A Honda Civic 2008 with a LASFIT L1 LED headlamp [16] is used as the transmitter. A photodetector from Thorlabs (PDA100A) [17] is used as the receiver and a RaspberryPi Model3B+ [18] is used as the processing module. A PiPlate (DAQC2plate) [19] is utilized as an analog-to-digital converter (ADC) in the proposed V2X system. All the parameters used in the experimental setting are stated in Table I. A 50 Ω BNC terminator is added to the PDA100A which, according to the datasheet of the photodetector in [17], decreases the reflections and improves the signal to noise ratio of the collected signal which will be between 0 V-5 V. In addition, the received light power will be a function of this collected signal and can be converted according to the amplifier mode and the wavelength of the visible light used [17]. A 335 nm-610 nm bandpass optical filter from Thorlabs is used to remove the effect of IR and lower wavelengths. The equation used to convert the received signal to the received light power is as follows [17]:

$$P_{in} = \frac{2V_{out}}{R_{PDA100A}(\lambda)G(G_{amp})}, \tag{1}$$

where P_{in} is the received light power at the PD (watts), V_{out} is the output signal from the ADC (V), $R_{PDA100A}(\lambda)$ is the PDA100A responsivity to different wavelengths which

TABLE I
PARAMETERS USED IN DATA COLLECTION EXPERIMENTAL SETTING

Parameter	Value
Transmitter (Tx) LED	Honda Civic 2008 with a LASFIT (L1 9005) LED
Receiver (Rx) PD	Thorlabs PDA100A
Receiver detection area	$10\,\text{mm}^2$
Avg. Tx power (electrical)	20 Watts
Tx and Rx Height	60 cm
ADC (DAQC2plate)	$366\,\mu V$ per bit, up to $12\,V$ input range, and 50 KHz samples per sec

is 0.4 Amp/watt for 610 nm wavelength, and $G(G_{amp})$ is the transimpedance gain (V/Amp) which will vary according to the chosen amplifier variable gain (G_{amp}) (from 0 dB to 70 dB). Equation (1) according to [17] can be simplified as:

$$[P_{in}]_{dBW} = 10\log_{10}(V_{out}) - 0.5G_{amp} - 21.76, \tag{2}$$

where $[P_{in}]_{dBW}$ is the received light power at the PD in dBW scale.

A Python script is used to collect the data samples and save them on the RaspberryPi. Finally, offline data processing is done on a laptop using MATLAB scripts.

III. Proposed Channel Model

The visible light channel has been studied intensively in the context of indoor communications [1], [2]. One of the most used and adopted line-of-sight (LOS) channel models is Lambertian model [20]. The Lambertian model presents the effects of different variables and parameters that make the visible light signal vary at the receiver end. The parameters are the transmitter power, the distance between light source and PD, optical PD size, PD field of view (FOV) (which is the region of space where the detector can detect any light entering it) and the incident angle (θ). The Lambertian model for the received signal power-distance relation is given as follows:

$$P_r = \frac{(n+1)A_R P_t}{2\pi D^{\gamma}} \cos^n(\phi)\cos(\theta), \forall \theta < \phi_{1/2}, \tag{3}$$

where P_t is the transmitter power in watts, P_r is the received signal power in watts and A_R is the optical detector size. ϕ and θ are angles of irradiance and incidence, respectively. The path loss exponent γ depends on the environmental conditions, such as reflectiveness of materials, light conditions, etc. Typically, the range of path loss exponent lies between 1 and 6.

In addition, $\phi_{1/2}$ is the semi-angle at half-power of the LED (which is half of the FOV of the light source), and n is the order of the Lambertian model and is given by

$$n = -\frac{\ln(2)}{\ln(\cos\phi_{1/2})}. \tag{4}$$

In our case, the light source and the receiver have the same movement directions and at the same height, therefore,

$$\theta = \phi, \tag{5}$$

where $0 < \theta < \phi_{1/2}$. Using (5), (3) can be further simplified as

$$P_r = \frac{(n+1)A_R P_t}{2\pi D^{\gamma}} \cos^{n+1}(\theta). \tag{6}$$

Then, in order to derive $P_r(t)$ in terms of $D(t)$, (6) is further simplified by defining a constant K as

$$K = \frac{(n+1)A_R P_t}{2\pi}. \tag{7}$$

Which leads to,

$$P_r = KD^{-\gamma}\cos^{n+1}(\theta). \tag{8}$$

Taking $10\log_{10}(.)$ at both sides,

$$P_{r_{dB}} = K_{dB} - \gamma D_{dB} + 10(n+1)\log_{10}(\cos(\theta)), \tag{9}$$

where $P_{r_{dB}} = 10\log_{10}(P_r)$, $K_{dB} = 10\log_{10}(K)$, and $D_{dB} = 10\log_{10}(D)$.

It is given that $\cos(\theta) = \frac{R}{D} = \frac{\sqrt{D^2 - w^2}}{D} = \sqrt{1 - \frac{w^2}{D^2}}$. Hence,

$$P_{r_{dB}} = K_{dB} - \gamma D_{dB} + 5(n+1)\log_{10}\left(1 - \frac{w^2}{D^2}\right). \tag{10}$$

Finally, the expression can be divided into two conditions:

$$P_{r_{dB}} = \begin{cases} K_{dB} - \gamma D_{dB}, & \frac{w^2}{D^2} << 1 \\ K_{dB} - \gamma D_{dB} + G_{dB}, & \text{otherwise} \end{cases} \tag{11}$$

where $G_{dB} = 5(n+1)\log_{10}\left(1 - \frac{w^2}{D^2}\right)$. The first condition (far-scenario) is when D is large enough or when w is small, which can also be called as log-linear simplified model as $P_{r_{dB}} = K_{dB} - \gamma D_{dB} \rightarrow P_r = KD^{-\gamma}$. While the second condition (near-scenario) is when D is small or when w is large compared to D.

Notice that for a constant value of K_{dB} and γ, the received power changes with the distance. The longer the distance between the transmitter (light source, e.g. LED) and receiver (PD), the lower the received power is and a factor G_{dB} is added in near-scenarios.

IV. Measurement Results and Verification

In this section, the data collected from the setting presented in Fig. 2 in both static and dynamic channel modeling scenarios are presented. In case of dynamic channel modeling, data for both night and daylight environments are presented.

A. Static Channel Modeling Scenario

In the static scenario, measurements were conducted with the car stationary at various knwon distances from the PD. In Fig. 3, the channel model is estimated after measuring the received power at several distance points at night and fitting the collected measurement values to estimate the best channel model parameters to fit the data. As shown in Fig. 3, the

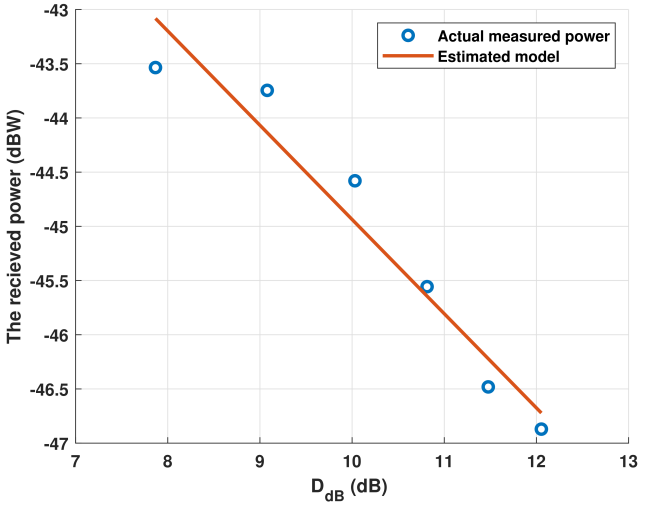

Fig. 3. Static channel model with vehicle equipped with LED headlamps (night scenario measurements).

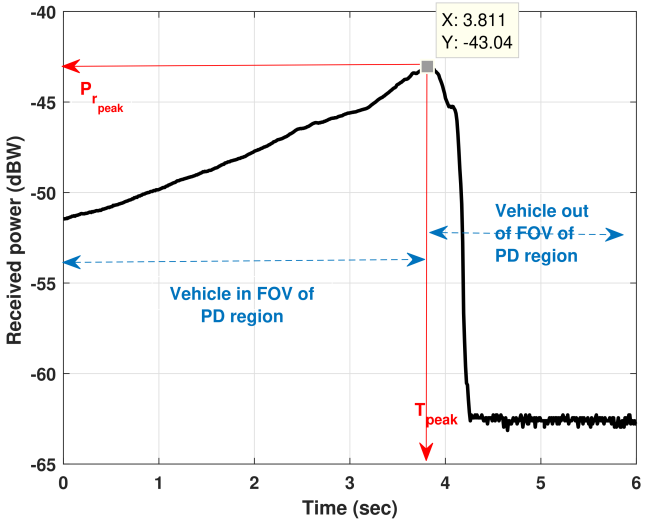

Fig. 4. Received power (dB) at night versus time (sec) with vehicle equipped with normal headlamps.

data is collected on multiple distances between (8 m-12 m) with 200 samples averaged at each point (2 seconds of data at 100 samples/sec sampling rate). As the distance increased, the received power decreased at an exponential rate of γ. It is evident that the measurements at different distance points do not provide a complete picture of how the channel model is changing and behaving over different regions explained in Section III. However, one can observe that the linearity of the figure starts decreasing when $D_{dB} < 10$. Therefore, continuous measurements while vehicle approaching towards the PD would provide a better picture for realistic visible light channel modeling, which is discussed in the next section.

B. Dynamic Channel Modeling Scenario

The dynamic channel modeling is followed to overcome the limitations discussed in the previous subsection. It involves the car moving towards the photodetector at a known constant speed throughout the measurement process. The received light power at the PD is collected for a vehicle approaching the PD with a speed $V = 20$ mph (8.9408 m/sec) as shown in Fig. 1. The data is collected for 10 seconds with a sampling rate of 100 samples/sec (total of 1000 samples). After identifying the range (R) where the peak of the received power happens (R_{peak}) and saving it as a reference, the peak of the data saved is located as shown in Fig. 4. Then, the curve is flipped and the power value corresponding to each distance point is identified using the timing information. Therefore, the range (R) of each data point is calculated as follows:

$$R_i = R_{Peak} + V(T_{Peak} - t_i), \tag{12}$$

where R_i is the range (horizontal distance between vehicle and PD, T_{Peak} time stamp of the data point where the peak is measured, and t_i is the time stamp of each data point measured.

Additional details for the channel modeling experimental setup are as follows:

- The vehicle is moving at a known constant speed (V).
- Vertical distance of the vehicle from PD (w) is also constant and known.
- The range (R) at which the peak power is received at PD is known.

After transforming the time axis with range (R) or actual distance (D) axis using (12), the channel model can be estimated using linear fitting as shown in $P_{r_{dB}} = K_{dB} - \gamma D_{dB}$.

Fig. 5 illustrates the fluctuation of received power (in dBW) in relation to the distance (in dB) at night for 5 distinct test cases. The graph also includes a linear fit for scenarios involving greater distances. It is clear from this graph that the linear region of the channel model starts when $D_{dB} > 10$. When the range is less, the channel behavior appears to be non-linear which is because of G_{dB} in equation (11) (when condition $\frac{w^2}{D^2} << 1$ is not satisfied). In addition, Fig. 6 displays the received power vs. distance graph during sunny daylight for 5 test runs. It can be observed that there is a difference in received light power at night and sunny daylight scenarios, even though the linear region starts $D_{dB} > 10$ for both. In daylight scenario (Fig. 6), the power received by the PD is higher and more susceptible to noise due to additional interference from sunlight.

V. Conclusions

This study analyzed and validated a mathematically more tractable path loss channel model that can be used for vehicular sensing and communication applications. According to the developed model, when the incident angle of light at the receiver was small, the received light power became linear with respect to logarithmic distance between the transmitter and the receiver. The model was validated by a set of experimental measurements in both static and dynamic scenarios, and in both night and daytime settings. This proposed model can be utilized in multiple visible light enabled sensing and

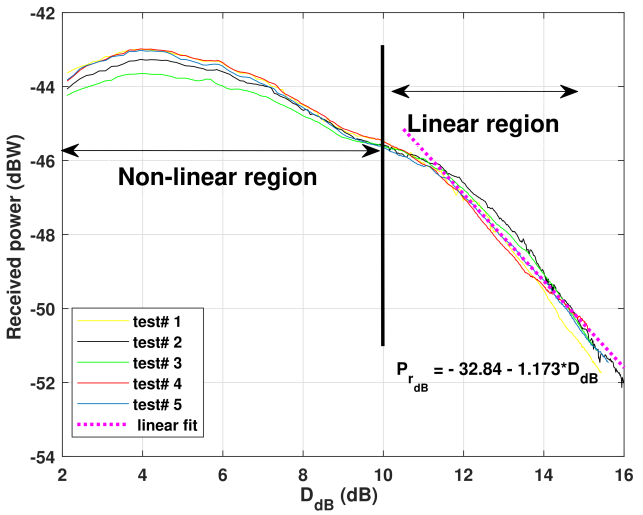

Fig. 5. Received power (dBW) at night versus distance in log domain (dB) for different test cases and expression for linear region with $K_{dB} = -32.84$ and $\gamma = 1.173$.

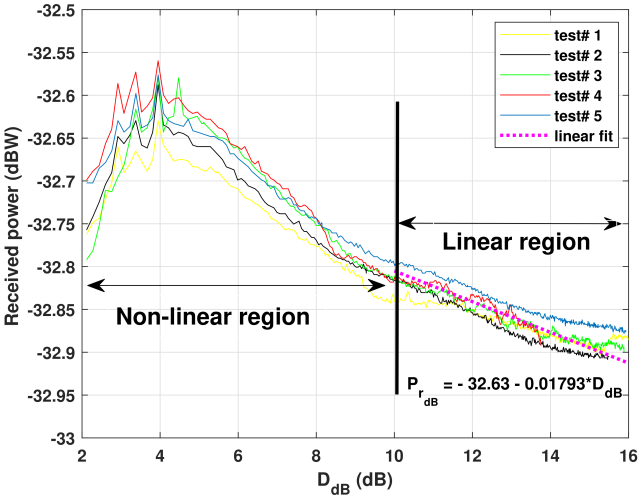

Fig. 6. Received power (dBW) at sunny daylight versus distance in log domain (dB) for different test cases and expression for linear region with $K_{dB} = -32.63$ and $\gamma = -0.01793$.

communication applications where reduction of the complexity of the channel model is needed.

REFERENCES

[1] D. Karunatilaka, F. Zafar, V. Kalavally, and R. Parthiban, "LED based indoor visible light communications: State of the art," *IEEE Communications Surveys Tutorials*, vol. 17, no. 3, pp. 1649–1678, thirdquarter 2015.

[2] P. H. Pathak, X. Feng, P. Hu, and P. Mohapatra, "Visible light communication, networking, and sensing: A survey, potential and challenges," *IEEE Communications Surveys & Tutorials*, vol. 17, no. 4, pp. 2047–2077, 2015.

[3] S. Rajagopal, R. D. Roberts, and S. K. Lim, "IEEE 802.15.7 visible light communication: modulation schemes and dimming support," *IEEE Communications Magazine*, vol. 50, no. 3, pp. 72–82, March 2012.

[4] C. B. Liu, B. Sadeghi, and E. W. Knightly, "Enabling vehicular visible light communication (V2LC) networks," in *Proceedings of the Eighth ACM International Workshop on Vehicular Inter-networking*, ser. VANET '11. New York, NY, USA: ACM, 2011, pp. 41–50. [Online]. Available: http://doi.acm.org/10.1145/2030698.2030705

[5] A. Cailean, B. Cagneau, L. Chassagne, S. Topsu, Y. Alayli, and J. Blosseville, "Visible light communications: Application to cooperation between vehicles and road infrastructures," in *2012 IEEE Intelligent Vehicles Symposium*, June 2012, pp. 1055–1059.

[6] N. Lourenco, D. Terra, N. Kumar, L. N. Alves, and R. L. Aguiar, "Visible light communication system for outdoor applications," in *2012 8th International Symposium on Communication Systems, Networks Digital Signal Processing (CSNDSP)*, July 2012, pp. 1–6.

[7] Y. Qiu, H.-H. Chen, and W.-X. Meng, "Channel modeling for visible light communications—a survey," *Wireless Communications and Mobile Computing*, vol. 16, no. 14, pp. 2016–2034, 2016.

[8] H. Abuella, F. Miramirkhani, S. Ekin, M. Uysal, and S. Ahmed, "ViLDAR–visible light sensing-based speed estimation using vehicle headlamps," *IEEE Transactions on Vehicular Technology*, vol. 68, no. 11, pp. 10 406–10 417, 2019.

[9] K. Cui, G. Chen, Z. Xu, and R. D. Roberts, "Traffic light to vehicle visible light communication channel characterization," *Appl. Opt.*, vol. 51, no. 27, pp. 6594–6605, Sep 2012.

[10] W. Viriyasitavat, S. Yu, and H. Tsai, "Short paper: Channel model for visible light communications using off-the-shelf scooter taillight," in *2013 IEEE Vehicular Networking Conference*, Dec 2013, pp. 170–173.

[11] B. Turan, G. Gurbilek, A. Uyrus, and S. C. Ergen, "Vehicular vlc frequency domain channel sounding and characterization," in *2018 IEEE Vehicular Networking Conference (VNC)*, Dec 2018, pp. 1–8.

[12] L. Cheng, W. Viriyasitavat, M. Boban, and H. Tsai, "Comparison of radio frequency and visible light propagation channels for vehicular communications," *IEEE Access*, vol. 6, pp. 2634–2644, 2018.

[13] H. B. Eldeeb, F. Miramirkhani, and M. Uysal, "A path loss model for vehicle-to-vehicle visible light communications," in *2019 15th International Conference on Telecommunications (ConTEL)*, 2019, pp. 1–5.

[14] M. Elamassie, M. Karbalayghareh, F. Miramirkhani, R. C. Kizilirmak, and M. Uysal, "Effect of fog and rain on the performance of vehicular visible light communications," in *2018 IEEE 87th Vehicular Technology Conference (VTC Spring)*, 2018, pp. 1–6.

[15] A. Memedi, C. Tebruegge, J. Jahneke, and F. Dressler, "Impact of vehicle type and headlight characteristics on vehicular vlc performance," in *2018 IEEE Vehicular Networking Conference (VNC)*, Dec 2018, pp. 1–8.

[16] "LASFIT (L1 9005) LED)," Accessed: 2018. [Online]. Available: www.lasfit.com

[17] "Photo-detector (Thorlabs) PDA-100A," Accessed: 2018. [Online]. Available: www.thorlabs.com

[18] "RaspberryPi (miniature computer)," Accessed: 2018. [Online]. Available: www.raspberrypi.org

[19] "Pi-Plates (DAQC2plate)," Accessed: 2018. [Online]. Available: www.pi-plates.com

[20] F. R. Gfeller and U. Bapst, "Wireless in-house data communication via diffuse infrared radiation," *Proceedings of the IEEE*, vol. 67, no. 11, pp. 1474–1486, Nov 1979.